2019 IMEKO TC-4 International Conference on
Metrology for Archaeology and Cultural Heritage
Florence, Italy, December 4-6, 2019

An innovative structural health monitoring system for the preliminary study of an ancient anti-seismic construction technique.

Carmelo Scuro[1], Domenico L. Carnì[2], Francesco Lamonaca[3], Renato S. Olivito[4], Gabriele Milani[5]

[1] *Department of Physics, University of Calabria, Rende (CS), Italy, carmelo.scuro@unical.it*
[2] *Department of Informatics, Modelling, Electronics and Systems Science, University of Calabria, Rende (CS), Italy, dlcarni@dimes.unical.it*
[3] *Department of Engineering, University of Sannio Benevento (BN), Italy, flamonaca@unisannio.it*
[4] *Department of Civil Engeneering, University of Calabria, Rende (CS), Italy, renato.olivito@unical.it*
[5] *Department of Architecture, Built Environment and Construction Engineering, Technical University of Milan, Milan, Italy, gabriele.milani@polimi.it*

***Abstract* – The Italian historical and cultural heritage is one of the most interesting and great in the world. The study of this heritage patrimony is bringing new discovery in the field of structural science. An ancient anti-seismic structure was discovered in Calabria region. Such structure is based on fictile tubules bricks a still not well studied construction method. In this paper we propose an innovative measurement method to investigate the mechanical properties of this anti-seismic structures.**

I. INTRODUCTION

In the investigation of the safety of historical structures is important to determine information about the action of the environment, the materials quality, the evolution of the alteration in a single part or in the whole structure caused by the materials aging and accidental events [1-2].

Whit this aim, the Structural Health Monitoring (SHM) systems permit to identify, characterize and detect the degradation and damage of different types of engineering structures and in particular the historical constructions. These systems are composed by an acquisition and elaboration system connected proper sensors for the evaluation of different physical quantity. The main information provided by the SHM systems are: acceleration, temperature, tensile and compressive stress humidity and so on [3]. Typically, the methods used in SHM are non-invasive with the deployment of sensors in specific checkpoints (established by the experts). The information acquired with the sensors are merged with the mathematical models of the structure to determine the structure safety evolution [3].

The paradigm of Internet of Thighs (IoT) well fit to SHM [4]. In fact, in the IoT paradigm each node is equipped with sensing, data transmissions capability and processing. The information is transmitted using an Internet connection in the Cloud and are elaborated by distributed systems managed by a paradigm of Big Data [5].

The purpose of this paper is to start a preliminary study of a SHM to be applied to a structure made with not known construction technique such as fictile tubules bricks [6] technique.

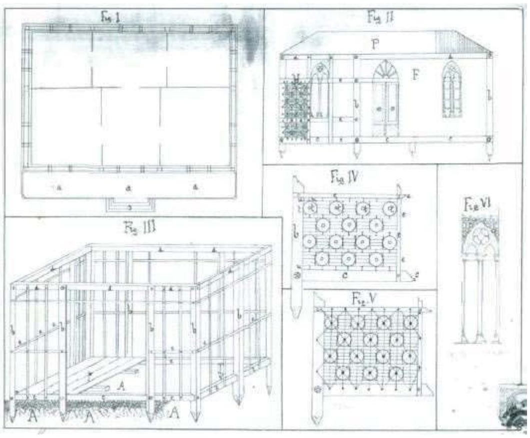

Fig. 1. Pasquale Frezza's patented design [8]

On 1908 a hugely disastrous earthquake, characterized by an estimated magnitude of 7 in Richter scale, destroyed the cities of Messina (Sicily) and Reggio Calabria. Most of the buildings in the two nearby cities collapsed, except those structures with a specific type of hollow clay bricks called fictile tubules [7]. In the process of reconstruction of Messina and Reggio Calabria, Pasquale Frezza, a Calabrian engineer, intended and patented a construction technique which evolved the concept of casa *baraccata* by including the use of fictile tubules in order to simply and quickly erect anti-seismic houses [8-9]. In particular, the new building technique alternating common bricks and fictile tubules, thus removing the diagonal bracing members consisted of masonry walls built within the timber frame as show in figure 1.

Fig. 2. Phases of preparation of the specimen

II. PREPARATION OF THE SPECIMEN

The dimensions of the specimen wall are 60×60×15 cm^3. The outer timber frame consists of four poplar beams with a cross-section of 15×3 cm^2). The connection between adjacent beams is ensured by cutting their extremities to make half-lap fastenings and then bolting them together with four iron screws. The common bricks employed have a square cross-section of 5.5 cm per side and a height of 13 cm. The fictile tubules are produced in a potter factory with innovative and faster techniques, and then refined on the potter's wheel. These elements and the mortar employed were tested and characterized in previous works [6;10]. They have the same height of the bricks (13 cm) and present a thickness of 6 mm (Fig. 2). The mortar is characterized by a compressive strength of about 2.5 MPa and corresponds to the one labelled as M2.5 bastarda according to Table 11.10.IV of the 2008 Italian Building Code. This particular mortar is composed by 9 parts of sand, 2 of lime mortar and 1 of cement.

A 2 cm thick layer of mortar to cover the bricks and the tips of the fictile tubules completes the specimen wall

III. DIAGONAL COMPRESSIVE TESTS

The diagonal compressive test on the unreinforced specimen was carried out by rotating the wall of 45°; two steel caps are placed on the specimen, one at top for uniformly distributing the load and the other at the bottom for support. The speed test is 0.5 mm/s. Two couples of transducers were applied to the wall to further monitor the relative displacements: those referred to as LVDT0 measure horizontal displacements between two fictile tubules, whereas those referred to as LVDT1 measure vertical displacements between bricks (Fig. 3). The test was stopped at the formation of the first damage and when the diagrams was arrived to the finish of a linear elastic branch. The recorded peak load is equal to 46 kN (Fig.5).

The shear strength of the wall S_s was evaluated as suggested by [11] using Eq. (1):

$$S_s = \frac{0{,}707 \cdot P}{A_n} \quad (1)$$

where, P is the peak load and A_n is the area which is evaluated according to Eq. (2):

$$A_n = \left(\frac{w+h}{2}\right) \cdot t \cdot n \quad (2)$$

w and *h* are respectively the width and the height of the specimen, *t* is the thickness of the specimen and *n* is a coefficient related to the rate of voids in the specimen (here considered equal to 0.6 where 1 corresponds to a wall with no voids). The shear strength corresponding to the peak loads is equal to 0.73 MPa.

Fig. 3. Test set up

When the first crack appeared in the specimen, the test was stopped, and the specimen was repaired and reinforced. Three Basalt-FRCM strips of 100 mm were placed at the side of the wall characterized by the layer of two cm of mortar (Fig. 4). In order to measure the strains on them, two strain gauges were applied at central strip in correspondence of the fibers perpendicular to the cracks. Then, the test was repeated on the reinforced specimen until collapse.

The maximum value of the load recorded during the reinforced test is equal to 66.48 kN (Fig. 5). At this load value, a failure of the Basalt-FRCM (B-FRCM) reinforcement occurred [12-13]. The collapse of the reinforcement strip happens through debonding with cohesive failure of the substrate (Fig. 6).

Fig. 4. Reinforcement of the specimen

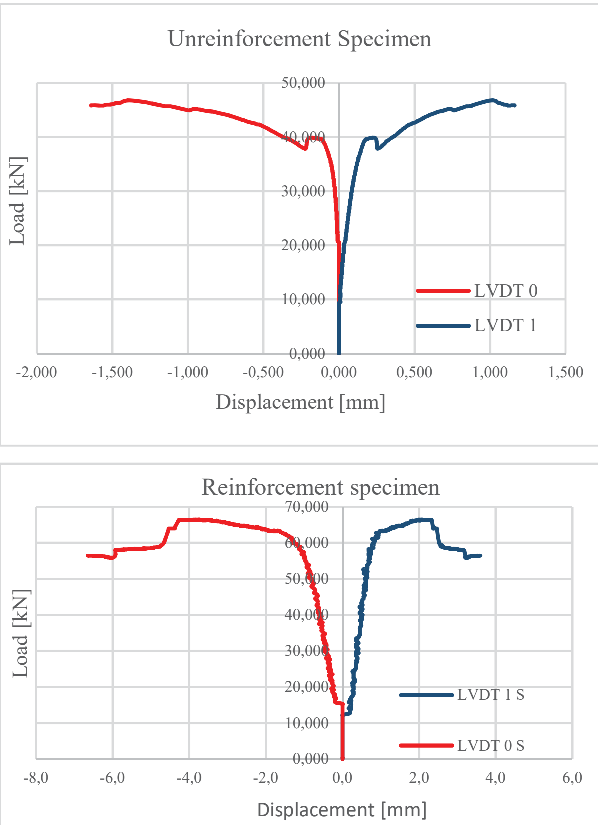

Fig. 5. Load vs Displacement diagrams of transducers for unreinforcement specimen (upper) and reinforced specimen (lower).

In order to obtain the value of the strain that occurred in the reinforced basalt fiber used to repair of the specimen, two strain gauges ware applied in central part of the diagonal BFRP as show in figure 7.

Fig. 6. Collapse of the reinforcement strip

A strain gauge is a device used to measure strain on an specimen subject to different type of stress, for example compression or tensile stress.

The strain gauges used in the test are the most common type and consists of an insulating flexible backing which supports a metallic foil pattern. The gauge is attached to the object by a cyanoacrylate. When the basalt fibers is deformed, the foil is deformed, causing its electrical resistance to change. This resistance change, usually measured using a Wheatstone bridge, is related to the strain by the quantity known as the Gauge factor.

Fig. 7. Strain gauges

Figure 9 shown the diagram Shear Stress vs Strain obtained during the test conducted on the reinforced specimen.

The Shear Stress was evaluated by eq.(1).

The average value of the deformation recorded during the test by the two strain gauges was 3.25 [µm/m] E-3. This value is in accordance with the value prescribed by the manufacturer of the fiber that certifies it among the 3- 3.5 [µm/m] E-3.

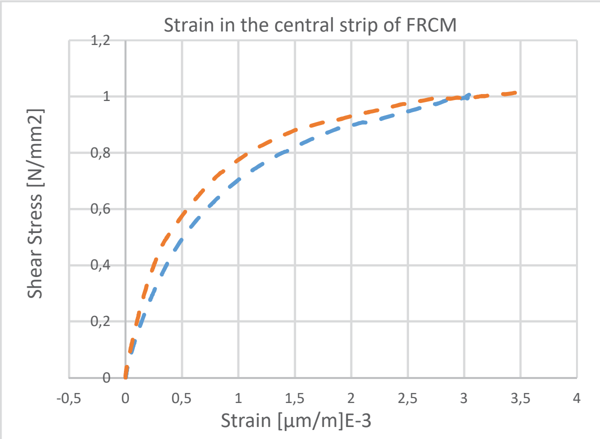

Fig. 8. Shear Stress vs Strain diagrams

IV. EXPERIMENTAL TESTBED

Two different Acquisition System (AS) was used in order to monitoring the displacements, in the case of unreinforced test, and the displacement and the strain of the basalt fibber in the case of reinforcement test.

The first AS was composed as following: two Linear Variable Differential Transformer (LVDT) [14], used for monitoring the horizontal and vertical displacement, were connected to data acquisition system (DAQ) Spider-8 which transmitted the data to a computer. The second was composed of the same LVDT and two strain gauges, which were connected at DAQ 5100B of System Micromeasurement. The second DAQ permits to acquire, in real time, two different types of data that were transmitted to a computer in order to processing them in real time.

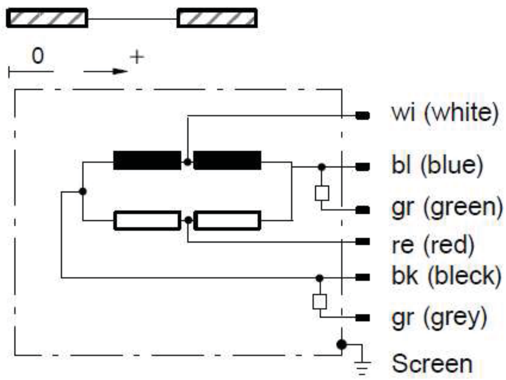

Fig. 9. Electronic scheme of LVDT WA-T [15]

The LVDTs used in order to monitoring the displacement in the masonry arch are procured by HBM and are of the type WA-T 50 mm. The displacement transducers WA-T are in probe version and they use an active quarter bridge circuit based on the differential inductor principle. The bridge is also directly integrated in the sensor to create a full bridge circuit for easy connection of the WA-T transducer to DAQ. The range of displacement that it is possible to measure with this type of LVDTs is 0-50 mm and the linearity variation in relation to nominal value is ±1%.

The strain gauges employed are of the type PFL-10-1. They are Polyester linear gauges with mild steel compensation. This is a foil strain gauge having polyester resin backing. It used for measurement on steel, concrete or mortar. All standard strain gauges come with 2 cm lead wires pre-attached. This type of strain gauges are characterized by: nominal resistance equal to 120 Ω, operetional temperature [20, 80]°C and Strain Limit of 2 % (20000 µstrain).

The DAQ, Spider 8, was used by an individual operator and has ensured: Simultaneous measurement acquisition, high sampling rate at 16-bit resolution and selectable digital filters. The linearity variation in relation to nominal value is ±0.05 %, as a consequence it is negligible in the evaluation of the measurement accuracy with respect to the sensor linear characteristic.

System 5000's Model 5100B Scanners acquire test data within 1 millisecond from up to 1200 channels at scan intervals as short as 0.02 s. This permits to have more accurate test results, and the ability to capture data under static loading conditions immediately before failure of the structure monitored. The Strain gauge cards integrated, include built-in bridge completion for quarter and half bridges, and a constant voltage power supply for 0.0, 0.5, 1.0, 2.0, 5.0, and 10.0 VDC bridge excitation. The A/D CONVERTER is characterized by 16-bit successive approximation converter with 40 µs total conversion time per reading.

The 5100B operate with 1 ms per scan. Fifty complete scans per second typical usage. Concurrent scanning for all scanners. Input channels in each single scanner are scanned sequentially at 0.04 ms intervals and stored in random access memory within a 1 ms window.

The main problem observed during this test was the return of the LVDT data during the reinforced test. As shown in figure 5 in the elastic branch of the load vs displacement graph there is a disturbance caused by a noise due to the DAQ. The data acquired instead by the channels dedicated to the strain gages do not present this problem. For this reason, a spline fitness function has been implemented to minimize the effect of the noise preserving the shape of the Load vs Displacement diagram, obtaining new graphs shown in figure 10. In particular, the cubic spline interpolation algorithm is used on the acquired data. The spline function smooth the random trend due to the noise, permitting to highlight the trend of the load vs the displacement.

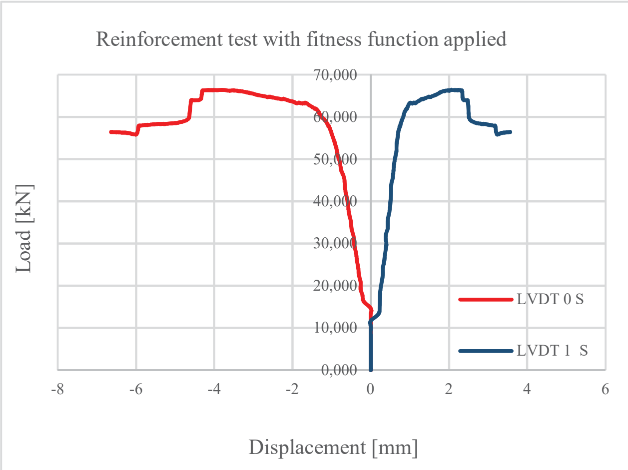

Fig. 10. Load vs Displacement diagrams after the application of fitness function

REFERENCES

[1] F.Lamonaca, P.F.Sciammarella, C.Scuro, D.L.Carnì, R.S.Olivito (2018, April). Internet of things for structural health monitoring. In 2018 Workshop on Metrology for Industry 4.0 and IoT (pp. 95-100). IEEE.

[2] F.Lamonaca, P.F.Sciammarella, C.Scuro, D.L.Carnì, R.S.Olivito (2018, April). Synchronization of IoT layers for structural health monitoring. In 2018 Workshop on Metrology for Industry 4.0 and IoT (pp. 89-94). IEEE.

[3] C.Scuro, P.F.Sciammarella, F.Lamonaca, R.S.Olivito, D.L.Carnì (2018). IoT for structural health monitoring. IEEE Instrumentation & Measurement Magazine, 21(6), 4-14.

[4] J.Gubbi, R.Buyya, S.Marusic and M.Palaniswami. (2013). Internet of Things (IoT): A vision, architectural elements, and future directions. Future generation computer systems, 29(7), 1645-1660.

[5] R.Kitchin. (2014). Big Data, new epistemologies and paradigm shifts. Big Data & Society, 1(1), 2053951714528481.

[6] C.Scuro, S.Tiberti, R.Codispoti, G.Milani, R.S.Olivito. Fictile tubules: A traditional Mediterranean construction technique for masonry vaulted systems. Construction and Building Materials, 193 (2018), 84-96.

[7] C.Scuro, F.Lamonaca, R.Codispoti, D.L.Carnì, & R.S. (2018). Experimental and numerical analysis on masonry arch built with fictile tubules bricks. Measurement, 130, 246-254.

[8] S.Tiberti, C.Scuro, R.Codispoti, R.S.Olivito, G.Milani. (2019). Experimental and numerical analysis of historical aseismic construction system. In Structural Analysis of Historical Constructions (pp. 910-918). Springer, Cham.

[9] Olivito, R. S., Codispoti, R., & Scuro, C. (2017, November). A seismic analysis for masonry constructions: The different schematization methods of masonry walls. In AIP Conference Proceedings (Vol. 1906, No. 1, p. 090007). AIP Publishing.

10] S.Tiberti, C.Scuro, R.Codispoti, R.S.Olivito, G.Milani. (2017, November). Masonry structures built with fictile tubules: Experimental and numerical analyses. In AIP Conference Proceedings (Vol. 1906, No. 1, p. 090010). AIP Publishing.

[11] American Society for Testing and Materials (2015) ASTM E519 / E519M-15, Standard Test Method for Diag-onal Tension (Shear) in Masonry Assemblages. doi: 10.1520/E0519_E0519M-15.

[12] Olivito, R. S., Codispoti, R., Scuro, C., & Porzio, S. (2018). Experimental evaluation of the adhesion of a FRCM-tuff strengthening system. Procedia Structural Integrity, 12, 594-601.

[13] Olivito, R. S., Codispoti, R., Scuro, C., & Porzio, S. (2018). Experimental evaluation of the adhesion of a FRCM-tuff strengthening system. Procedia Structural Integrity, 12, 594-601.

[14] P.Antunes, H.Lima, H.Varum, P.André. Optical fiber sensors for static and dynamic health monitoring of civil engineering infrastructures: Abode wall case study, (2012) Measurement: Journal of the International Measurement Confederation, 45 (7), pp. 1695-1705.

[15] HBM LVDT WA-T Data sheet